A new fluorescent probe for distinguishing Zn(2+) and Cd(2+) with high sensitivity and selectivity

7 AUTHORS, INCLUDING:

Junkuo Gao
Zhejiang Sci-Tech University
59 PUBLICATIONS   **1,195** CITATIONS

SEE PROFILE

Jiancan Yu
Zhejiang University
56 PUBLICATIONS   **856** CITATIONS

SEE PROFILE

Yuanjing Cui
Zhejiang University
117 PUBLICATIONS   **3,451** CITATIONS

SEE PROFILE

Yu Yang
Zhejiang University
108 PUBLICATIONS   **1,860** CITATIONS

SEE PROFILE

PAPER

A new fluorescent probe for distinguishing Zn²⁺ and Cd²⁺ with high sensitivity and selectivity†

Yiqun Tan, Junkuo Gao, Jiancan Yu, Ziqi Wang, Yuanjing Cui, Yu Yang* and Guodong Qian*

A new fluorescence probe for distinguishing Zn²⁺ and Cd²⁺ is designed and synthesized. For the first time to our knowledge, this probe can recognize similar metal ions by coherently utilizing intramolecular charge transfer (ICT) and different electronic affinities of various metal ions, instead of by selective coordination alone, which may be interfered with and lose its selectivity easily in a complicated environment, providing a distinct recognition even by the naked eye for Zn²⁺ and Cd²⁺ with the sensitivity at the ppb level. This design strategy may initiate a straightforward approach for the selective detection of various metal ions with similar chemical properties in extensive applications such as environmental, industrial, and bio-science.

Introduction

In biological processes, Zn and Cd play distinct roles, although being group 12 elements, they have very similar chemical properties, such as electron configuration and coordination number. Zn²⁺ is the second most abundant transition metal ion in the human body and is crucial in gene transcription, regulation of metalloenzymes, neural signal transmission and apoptosis.[1–5] In contrast, Cd²⁺ may cause acute and chronic toxicity symptoms, or accumulate in organisms, resulting in certain forms of cancers and other diseases, although it has been widely used in agriculture, industry and the military for centuries.[6–10] Thus, extensive research efforts have been devoted to the quantitative measurement of trace Zn²⁺ and Cd²⁺.[11–13]

In recent years, fluorescent probes for metal ions have attracted much attention because of their advantages over other methods, such as high sensitivity, simplicity and real time detection.[14–18] Although many fluorescent sensors for the detection of Zn²⁺ and Cd²⁺ have been reported,[19–27] most of them have so far suffered from poor selectivity. Till today, the development of sensors that exhibit a distinct fluorescence response towards these two metal ions still remains challenging, which can be mainly ascribed to the contradiction between chemical properties and the sensing mechanism. Most of the probes designed for Zn²⁺ and Cd²⁺ detection to

date are based on the photo-induced electron transfer (PET) effect using di-2-picolylamine (DPA) as an ionophore for binding ions.[28,29] The fluorophores linked with DPA could be quenched by the PET effect and recovered after the combination of metal ions with DPA to shut off the PET effect.[30–32] The recognition capability of such probes relies on the selective coordination of ionophores with targeted ions.[33] Nevertheless, this sensing mechanism might lose its selectivity in the cases where species with similar binding characters were involved. This problem is very common not only in Zn²⁺/Cd²⁺, but also in Ca²⁺/Mg²⁺, Ag⁺/Hg²⁺ and K⁺/Na⁺. In 2009, Jiang *et al.* have developed a method for distinguishing Zn²⁺ and Cd²⁺ by introducing a carbonyl group.[34,35] However, this method also relies on the different coordination between Zn²⁺ and Cd²⁺ which restricts the use of it in the design of probes for other ions. New strategies for the design of probes which can recognize similar ions such as Zn²⁺ and Cd²⁺ are still desired.

To solve this problem, photo-induced ICT might be a good candidate. As a promising strategy, intramolecular charge transfer (ICT) was widely used in the design of fluorescence probes.[36–39] Probes based on ICT generally have structures containing an electron withdrawing group conjugated to an electron donating group, which permit ICT from the donor to the acceptor upon excitation,[40–42] accompanied by a large Stokes' shift associated with ICT efficiency. It is supposed that the interactions between targeted ions and the donor/acceptor group would affect the efficiency of ICT, leading to the variation of Stokes' shift and emission color, instead of only fluorescence switches for probes based on PET.[43–46] This interesting property may provide an efficient method for distinguishing similar ions because metal ions with different

State Key Laboratory of Silicon Materials, Cyrus Tang Center for Sensor Materials and Applications, Department of Materials Science and Engineering, Zhejiang University, Hangzhou, 310027, P. R. China. E-mail: gdqian@zju.edu.cn, yuyang@zju.edu.cn
†Electronic supplementary information (ESI) available. See DOI: 10.1039/c3dt50991e

electron affinities may introduce quite different influences on the ICT effect and Stokes' shift. However, to the best of our knowledge, few reports on probes based on the ICT effect capable of recognizing similar metal ions have been reported. In this work, we employ the ICT effect as a basic mechanism to design a new fluorescent probe, 2-(4-((4-([2,2′,6′,2″-terpyridin]-4′-yl)phenyl)ethynyl)phenyl)benzo-[*d*]thiazole (**ZC-F1**). Unlike the previously reported probes, the selectivity of this sensor relies not only on the specific coordination with metal ions, but also on the different electron affinities of the targeting metal ions. As a result, with this probe, one can readily tell Zn^{2+} and Cd^{2+} apart based on their different fluorescence emission colors. This design strategy may also initiate extensive research on the development of fluorescent probes for distinguishing other similar metal ions.

Experimental section

Reagents and apparatus

Solvents and reagents were obtained from commercial sources and used as received without further purification. ^{1}H NMR spectra were recorded in CDCl$_3$ on a 500 MHz Bruker Avance DMX500 spectrometer with tetramethylsilane (TMS) as an internal standard. Elemental analysis was performed using a Thermo Finnigan Flash EA1112 microelemental analyzer. Differential scanning calorimetry (DSC) was performed on a Netzsch Instruments 200 F3 at a heating rate of 10 K min^{-1} under a nitrogen atmosphere. Fluorescence emission spectra and excitation spectra were obtained on a Hitachi F4600 fluorescence spectrophotometer. UV-vis absorption spectra were obtained using a Perkin-Elmer Lambda spectrophotometer. The fluorescence decay curves were measured using an Edinburgh Instrument F900. Fluorescence quantum yield is measured with an integrating sphere on an Edinburgh Instrument F900. IR spectra were recorded by a Thermo Fisher Nicolet iS10 spectrometer with KBr pellets. All the theoretical calculations were performed based on density functional theory at the B3LYP/6-31G(d) level.[47,48] The solvent effect on molecular geometries was included by means of the polarizable continuum model (PCM).[49,50] Based on the optimized geometry, all the molecular orbitals were calculated at the same level. All the calculations were performed using Gaussian09 software.[51]

Synthesis of ZC-F1

2-(4-Bromophenyl)benzothiazole (1). 4-Bromobenzaldehyde (0.46 g, 2.5 mmol) was stirred into a solution of 2-aminothiophenol (0.31 g, 2.5 mmol) in triethyl phosphate (25 mL). After 10 minutes, acetic acid (2.5 mL) was added into the solution and stirred for a further 10 minutes at a temperature of 60 °C. Lead(IV) acetate (1.5 g, 3.4 mmol) was added with rapid stirring. After stirring for a further 30 minutes, the solution was cooled to room temperature and extracted with CH$_2$Cl$_2$. The organic phase was collected and the solvent was evaporated. The resulting black solid was purified by chromatography

using CH$_2$Cl$_2$ and petroleum (1 : 2) as an eluent to obtain a white solid **1** (0.46 g, 63%). ^{1}H NMR (500 MHz, CDCl$_3$): δ = 8.07 (d, 1H, *J* = 8.1 Hz, ArH), 7.96 (m, 2H, *J* = 6.8 Hz, ArH), 7.91 (d, 1H, *J* = 8.0 Hz, ArH), 7.63 (m, 2H, *J* = 6.9 Hz, ArH), 7.50 (s, 1H, ArH), 7.38 (m, 2H, *J* = 7.1 Hz, ArH). IR (KBr pellet, cm^{-1}): 1921w, 1667w, 1475s, 1455m, 1432s, 1395s, 1314s, 1288m, 1248s, 1225s, 1103m, 1067s, 1012s, 971s, 934m, 839s, 827s, 752s, 721s, 708s, 684s, 625m, 617s, 548s, 480s, 431m. Anal. Calcd for C$_{13}$H$_8$BrNS: C, 53.81; N, 4.83; H, 2.78. Found: C, 53.81; N, 4.82; H, 2.76. Mp: 132.7 °C.

4-(4-(Benzo-[*d*]thiazol-2-yl)phenyl)-2-methylbut-3-yn-2-ol (2). **1** (1.44 g, 5 mmol), Pd(PPh$_3$)$_2$Cl$_2$ (0.14 g, 0.2 mmol), 2-methyl-3-butyn-2-ol (1.26 g, 15 mmol) and CuI (0.038 g, 0.2 mmol) were added into a mixture of Et$_3$N (2 mL) and toluene (8 mL) and refluxed for 12 h. The solution was evaporated and purified by chromatography using CH$_2$Cl$_2$ and EtOAC (20 : 1) as an eluent, resulting in white crystal **2** (0.64 g, 44%). ^{1}H NMR (500 MHz, CDCl$_3$): δ = 8.06 (d, 1H, *J* = 8.1 Hz, ArH), 8.03 (d, 2H, *J* = 8.3 Hz, ArH), 7.92 (d, 1H, *J* = 7.9 Hz, ArH), 7.54 (t, 3H, *J* = 8.3 Hz, ArH), 7.40 (s, 1H, ArH), 2.06 (s, 1H, OH), 1.65 (s, 6H, CH$_3$). IR (KBr pellet, cm^{-1}): 3354s, 3057m, 2994m, 2976s, 2929m, 1481s, 1454m, 1433s, 1406s, 1372s, 1310s, 1277s, 1251m, 1230s, 1197m, 1185m, 1162s, 974s, 963s, 908m, 847s, 759s, 728s, 636m, 621m, 592m, 562s, 498m, 441s. Anal. Calcd for C$_{18}$H$_{15}$NOS: C, 73.69; H, 5.15; N, 4.77. Found: C, 73.40; H, 5.13; N, 4.78.

2-(4-Ethynylphenyl)benzo-[*d*]thiazole (3). A mixture of **2** (0.59 g, 2 mmol) and KOH (0.56 g, 10 mmol) in toluene (10 mL) was refluxed for 2 h. The solution was then extracted with CH$_2$Cl$_2$, and the organic phase was combined and evaporated. The resulting black solid was purified by chromatography using CH$_2$Cl$_2$ and petroleum (1 : 1) as an eluent, affording a light yellow solid (0.42 g, 94%). ^{1}H NMR (500 MHz, CDCl$_3$): δ = 8.06 (t, 3H, *J* = 8.5 Hz, ArH), 7.92 (d, 1H, *J* = 6.9 Hz, ArH), 7.62 (d, 2H, *J* = 8.3 Hz, ArH), 7.52 (m, 1H, *J* = 7.2 Hz, ArH), 7.41 (m, 1H, *J* = 7.1 Hz, ArH), 3.23 (s, 1H, C≡CH). IR (KBr pellet, cm^{-1}): 3274m, 1476w, 1455w, 1432m, 1404m, 1312m, 1289w, 1252m, 1225m, 1178w, 1111m, 1072w, 1014w, 972s, 933m, 856m, 847s, 832s, 771m, 755s, 724s, 694m, 659m, 622s, 556m, 522m, 499m, 441m. Anal. Calcd for C$_{15}$H$_9$NS: C, 76.57; N, 5.95; H, 3.86. Found: C, 76.48; N, 5.87; H, 4.14. Mp: 129.6 °C.

4′-(*p*-Bromophenyl)-2,2′,6′,2″-terpyridine (4). 4-Bromobenzaldehyde (1 g, 5.4 mmol) and 2-acetylpyridine (1.3 g, 10.8 mmol) were stirred into methanol (120 mL) followed by addition of NaOH (0.22 g, 5.4 mmol) and NH$_4$OH (30 mL). The mixture was refluxed for 36 h, and then cooled down to room temperature. The precipitate was filtered and washed using methanol and water to obtain a white powder (0.8 g, 40%). ^{1}H NMR (500 MHz, CDCl$_3$): δ = 8.78 (t, 4H, *J* = 12 Hz, ArH), 8.74 (d, 2H, *J* = 7 Hz, ArH), 7.97 (s, 2H, ArH), 7.85 (d, 2H, *J* = 8 Hz, ArH), 7.67 (d, 2H, *J* = 2 Hz, ArH), 7.44 (s, 2H, ArH). IR (KBr pellet, cm^{-1}): 1605s, 1584s, 1567s, 1541s, 1489s, 1468s, 1443s, 1409s, 1380s, 1074s, 1037s, 1007s, 990s, 888s, 821s, 786s, 733s, 703s, 660s, 627s, 615s, 575s, 497s, 476s, 449s, 420s. Anal. Calcd for C$_{21}$H$_{14}$BrN$_3$: C, 64.96; N, 10.82; H, 3.63. Found: C, 65.03; N, 10.79; H, 3.66.

2-(4-((4-([2,2′:6′,2″-Terpyridin]-4′-yl)phenyl)ethynyl)phenyl)-benzo-[*d*]thiazole (ZC-F1). **4** (1.55 g, 4 mmol) and **3** (0.94 g, 4 mmol) were dissolved in a mixture of Et$_3$N (4 mL) and toluene (16 mL). CuI (0.038 g, 0.2 mmol) and Pd(PPh$_3$)$_2$Cl$_2$ (0.14 g, 0.2 mmol) were stirred into the solution and heated at 80 °C for 12 h under an argon atmosphere. The resulting solution was evaporated and purified by chromatography using CH$_2$Cl$_2$ and petroleum as an eluent to yield a yellow solid **4** (1.2 g, 55%). ^{1}H NMR (500 MHz, CDCl$_3$): δ = 8.78 (t, 4H, J = 12.0 Hz, ArH), 8.74 (d, 2H, J = 6.9 Hz, ArH), 8.06 (t, 3H, J = 8.4 Hz, ArH), 7.97 (s, 2H, ArH), 7.85 (m, 3H, J = 8.1 Hz, ArH), 7.67 (d, 2H, J = 2 Hz, ArH), 7.62 (d, 2H, J = 7.0 Hz, ArH), 7.52 (m, 1H, J = 7.1 Hz, ArH), 7.41 (m, 3H, J = 7.9 Hz, ArH). IR (KBr pellet, cm^{-1}): 1603w, 1584m, 1566m, 1541w, 1479m, 1466m, 1419w, 1388m, 967w, 824m, 790m, 762m, 733m, 684m, 659m, 644w, 622m, 558w, 536w, 496m, 442m. Anal. Calcd for C$_{36}$H$_{22}$N$_4$S: C, 79.68; N, 10.32; H, 4.09. Found: C, 79.46; N, 10.52; H, 4.13.
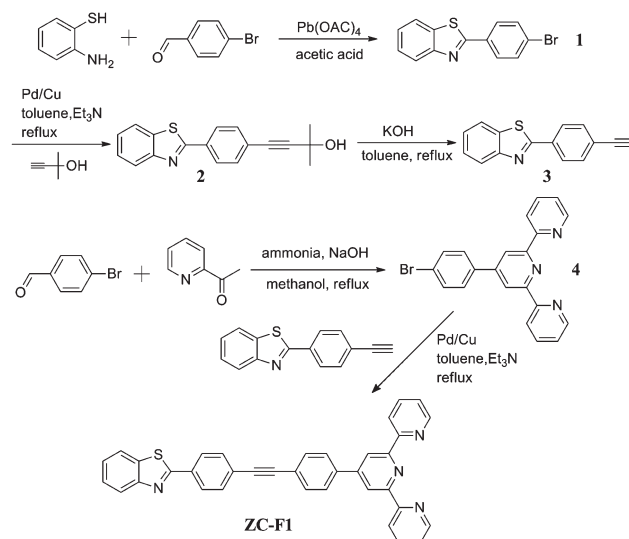
Scheme 1 Synthesis of the probe **ZC-F1**.

Results and discussion

Optimized design and synthesis of the probe ZC-F1

In the newly designed fluorescence probe, 2,2′,6′,2″-terpyridine is chosen as the coordination group instead of the commonly used DPA, and benzothiazole is selected as the acceptor for its strong electronic withdrawing ability, enlarged conjugated system and good photostability. The acceptor and coordination group is linked with phenylethynyl as the conjugated bridge. Thus, the ICT effect is expected in this probe.[52,53] After combining with metal ions, the energy level of the ICT state is supposed to be reduced, leading to both spectra shift and fluorescence intensity variation.[54] The crucial point is that the reducing degree of the ICT state is related to the electron withdrawing ability of metal ions, thereby even minor electronic differences between cations may cause quite a significant spectra shift. Thus, distinguishing Zn^{2+} and Cd^{2+} based on the same coordination can be expected.

As shown in Scheme 1, the compound **ZC-F1** can be synthesized in several steps from commercially available chemicals in high yield. Details of the synthesis are described in the Experimental section and the main photophysical parameters are listed in the ESI (Fig. S1, S2 and Table S1†).

Fluorescence response of the probe ZC-F1

To verify the feasibility of **ZC-F1** for distinguishing, the fluorescence emission spectrum of **ZC-F1** and its response towards Zn^{2+} and Cd^{2+} at various concentrations were first studied in acetonitrile solution at 0.45 μM, as shown in Fig. 1. The probe **ZC-F1** exhibits a broadband fluorescence emission spectrum with split peaks at 380 and 400 nm, respectively, which may be ascribed to the enlarged conjugated system of benzothiazole. With the titration of Zn^{2+}, the initial fluorescence bands gradually disappear and a new emission peak at 495 nm owing to the combination of the probe and Zn^{2+} is observed. A similar tendency is also observed with the titration of Cd^{2+} into the
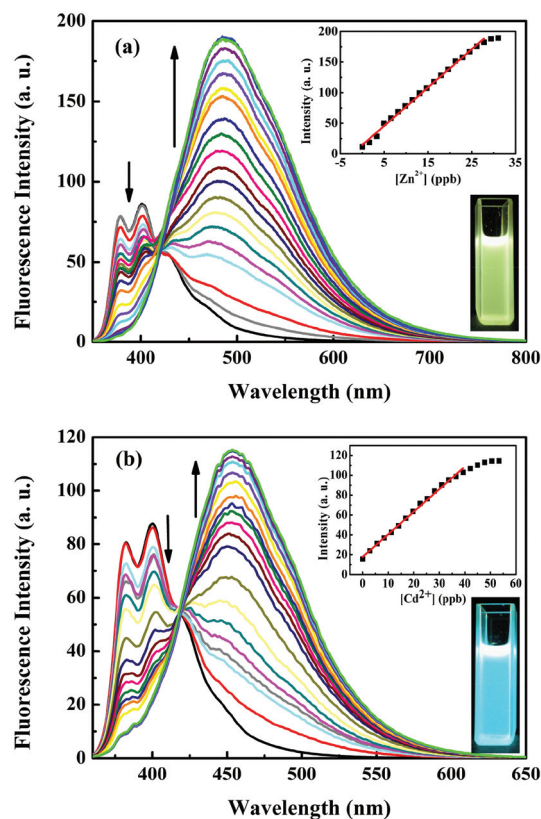

Fig. 1 Fluorescence emission spectra of **ZC-F1** (0.45 μM) excited at 341 nm upon titration of Zn^{2+} at the concentrations of 0, 1.63, 3.27, 4.90, 6.54, 8.17, 9.81, 11.44, 13.08, 14.71, 16.35, 17.98, 19.61, 21.25, 22.88, 24.52, 26.15, 27.79, 29.42, 31.06 ppb (a) and Cd^{2+} at the concentrations of 0, 2.81, 5.62, 8.43, 11.24, 14.05, 16.86, 19.67, 22.48, 25.29, 28.10, 30.91, 33.72, 36.53, 39.34, 42.15, 44.96, 47.77, 50.58, 53.40 ppb (b). Insets: fluorescence intensity as a function of the [Zn^{2+}] (a)/[Cd^{2+}] (b) and luminescent photos of **ZC-F1** titrated with Zn^{2+} (a)/Cd^{2+} (b) under excitation under a 315 nm UV lamp.
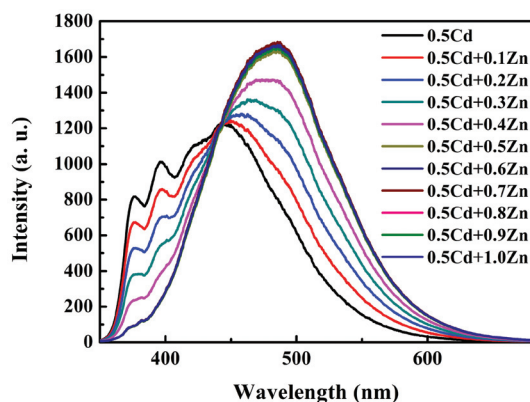
Fig. 2 Fluorescence emission spectra (excited at 341 nm) of **ZC-F1** (4.5 μM) with Cd^{2+} (0.5 equiv.) upon titration of Zn^{2+} (0.1, 0.2, 0.3, 0.4, 0.5, 0.6, 0.7, 0.8, 0.9 and 1.0 equiv.).

acetonitrile solution of **ZC-F1**. The most important feature is the shift in fluorescence emission peaks of **ZC-F1** to 455 nm after the addition of Cd^{2+}, which is 40 nm apart from that of **ZC-F1** titrated with Zn^{2+}, leading to different emission colors, *i.e.* blue for Cd^{2+} and green for Zn^{2+}. This result demonstrates that the probe can readily distinguish Zn^{2+} and Cd^{2+}. It is worth noting that the fluorescence intensity of **ZC-F1** has well fitted linear relationships with $[Zn^{2+}]/[Cd^{2+}]$ and a significant enhancement of fluorescence intensity can be observed even when $[Zn^{2+}]$ and $[Cd^{2+}]$ are as low as 25 nM, which is equal to 1.63 and 2.81 ppb respectively, indicating that **ZC-F1** is highly sensitive for Zn^{2+} and Cd^{2+} even at the ppb level.

Based on the titration study mentioned above, the association constants (log K_a) of the probe **ZC-F1** for Zn^{2+} and Cd^{2+} are found to be 3.75 and 3.62 (Fig. S3†) respectively, suggesting that the probe has almost the same chelated strength with Zn^{2+} and Cd^{2+}, which do favor reducing the interruption from each other. To further confirm this, we conducted a competitive experiment by titrating Zn^{2+} into the solution of **ZC-F1** subsaturated with Cd^{2+}. As shown in Fig. 2 and S4,† a red shift of the emission peak from 455 nm to 495 nm is observed with the addition of Zn^{2+}. When the probe is saturated by addition of 0.5 equiv. of Zn^{2+}, further titration of Zn^{2+} will not induce a spectra change, indicating no competition between Zn^{2+} and Cd^{2+}. It is worth noting that the fluorescence intensity at 455 nm shows no variation, indicating that the probe can detect Cd^{2+} quantitatively in the presence of Zn^{2+}. This result implies that this probe can be used to detect Zn^{2+} and Cd^{2+} when both of them are presented. Job's plot is also performed to confirm the possible binding modes of **ZC-F1** with Zn^{2+}/Cd^{2+} and certify a 1 : 1 stoichiometry (Fig. S5†).

Selectivity

To test the application of this probe in a complicated environment, representative interferences of biological and environmental interests such as Hg^{2+}, Ag^+, Fe^{3+}, Na^+, N_2H_4, Ca^{2+}, Pb^{2+}, Al^{3+}, Co^{2+}, Cu^{2+} and K^+ are introduced to investigate their impact on the selectivity of **ZC-F1** towards Zn^{2+} and Cd^{2+}. As
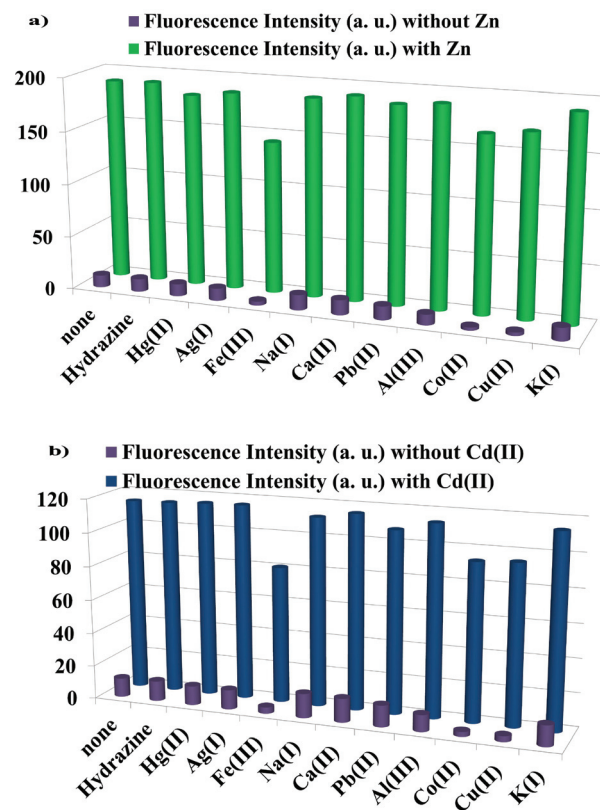

Fig. 3 Fluorescence response of **ZC-F1** (0.45 μM in acetonitrile) towards Zn^{2+} at 495 nm (a), Cd^{2+} at 455 nm (b) and various interferences (40 equiv. for K^+, Ca^{2+}, Na^+ and Al^{3+} and 20 equiv. for others) upon excitation at 341 nm.

shown in Fig. 3, addition of main group metal ions, including K^+, Ca^{2+}, Na^+ and Al^{3+}, exerts no effect on the fluorescence intensity before and after treating **ZC-F1** with Zn^{2+} or Cd^{2+}, whereas Fe^{3+}, Co^{2+}, Cu^{2+} and Pb^{2+} quench the fluorescence slightly. In addition, Hg lies in the same group as Zn and Cd, but Hg^{2+} and its common interference Ag^+ exhibit no disturbance. Moreover, hydrazine, which is known to be a highly reactive base and reducing agent, has no impact on the recognition, either. Thus, the good selectivity of **ZC-F1** is confirmed.

Theoretical calculations

To gain insight into the probing mechanism, computations on the probe before and after combination with Zn^{2+} and Cd^{2+} were performed based on density functional theory (DFT).

As shown in Fig. 4, electrons are mainly localized on the fluorophore at both the ground and excited states, while the two end-capped pyridine rings did not participate in the rearrangement of electrons, indicating that the charge transfer effect is quite weak, which can also be confirmed by the double-exponential fluorescence decay curves (Fig. S1 and Table S1†). Meanwhile, the pyridine rings and the other part of the molecule are not coplanar, which might be ascribed to the twist enforced by steric factors. However, after combining with Zn^{2+}, the electrons mainly localized on the fluorophore part in the ground state and the terpyridine part in the excited
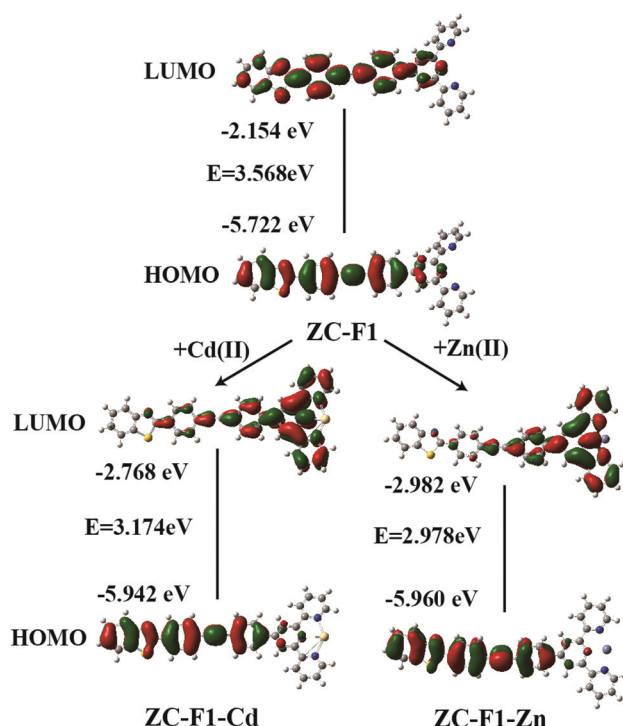
Fig. 4 HOMO–LUMO energy levels and the interfacial plots of the molecular orbitals for **ZC-F1** and its complex form with Zn^{2+} (**ZC-F1-Zn**) and Cd^{2+} (**ZC-F1-Cd**).

state respectively, which suggests that a strong ICT effect occurs owing to enhancement of the terpyridine electron withdrawing ability from Zn^{2+}. The pyridine rings have the same orientation within the conjugated plane due to the combination with Zn^{2+}, which may also enhance the ICT effect by improving the conjugation. The same results can be obtained for **ZC-F1-Cd**, except for its lower degree of electron rearrangement, indicating a shorter Stokes' shift than that of **ZC-F1-Zn** as observed in the experiment. It is worth mentioning that the calculated energy gaps between HOMO and LUMO of **ZC-F1**, **ZC-F1-Cd** and **ZC-F1-Zn** are in good agreement with those obtained from the absorption spectra (Fig. S2†), confirming the consistency of the theoretical calculations. Thus, the sensing mechanism is clear. After combining with Zn^{2+} or Cd^{2+}, the terpyridine group localizes on the same phase and participates in the charge transfer, resulting in the enhanced ICT effect and red shift of the fluorescence emission spectra. During this process, the combined metal ions play an important role for they decide the degree of enhancement of the ICT effect, leading to different emission colors.

Conclusions

In summary, a new highly sensitive and selective fluorescent probe possessing a distinct emission response towards Zn^{2+} and Cd^{2+} was obtained. This probe shows potential usage in the quantitative detection of these ions at the ppb level. By using the ICT effect and employing metal ions as a part of the conjugated system, the probe can discriminate Zn^{2+} from Cd^{2+} independently of differences in coordination. The strategy developed will also initiate extensive research on the selective detection of other ions with similar chemical properties.

Notes and references

1 B. L. Vallee and K. H. Falchuk, *Phys. Rev.*, 1993, **73**, 79–118.
2 A. Voegelin, S. Pfister, A. C. Scheinost, M. A. Marcus and R. Kretzschmar, *Environ. Sci. Technol.*, 2005, **39**, 6616–6623.
3 J. M. Berg and Y. Shi, *Science*, 1996, **271**, 1081–1085.
4 X. Xie and T. G. Smart, *Nature*, 1991, **349**, 521–524.
5 C. J. Frederickson and A. I. Bush, *BioMetals*, 2001, **14**, 353–366.
6 A. M. S. Mendes, G. P. Duda, C. W. A. d. Nascimento and M. O. Silva, *Sci. Agric.*, 2006, **63**, 328–332.
7 G. Jiang, L. Xu, S. Song, C. Zhu, Q. Wu, L. Zhang and L. Wu, *Toxicology*, 2008, **244**, 49–55.
8 S. Satarug, J. R. Baker, S. Urbenjapol, M. Haswell-Elkins, P. E. B. Reilly, D. J. Williams and M. R. Moore, *Toxicol. Lett.*, 2003, **137**, 65–83.
9 C. B. Murray, D. J. Norris and M. G. Bawendi, *J. Am. Chem. Soc.*, 1993, **115**, 8706–8715.
10 T. Jin, Y. Lu and M. Nordberg, *Neurotoxicology*, 1997, **18**, 872–872.
11 A. N. Anthemidis and C.-P. P. Karapatouchas, *Microchim. Acta*, 2008, **160**, 455–460.
12 G. Kaya and M. Yaman, *Talanta*, 2008, **75**, 1127–1133.
13 A. C. Davis, C. P. Calloway Jr. and B. T. Jones, *Talanta*, 2007, **71**, 1144–1149.
14 W. Xuan, C. Chen, Y. Cao, W. He, W. Jiang, K. Liu and W. Wang, *Chem. Commun.*, 2012, **48**, 7292–7294.
15 M. Collot, C. Loukou, A. V. Yakovlev, C. D. Wilms, D. Li, A. Evrard, A. Zamaleeva, L. Bourdieu, J. F. Leger, N. Ropert, J. Eilers, M. Oheim, A. Feltz and J. M. Mallet, *J. Am. Chem. Soc.*, 2012, **134**, 14923–14931.
16 Y. Zhao, X. B. Zhang, Z. X. Han, L. Qiao, C. Y. Li, L. X. Jian, G. L. Shen and R. Q. Yu, *Anal. Chem.*, 2009, **81**, 7022–7030.
17 Y. Tan, J. Yu, Y. Cui, Y. Yang, Z. Wang, X. Hao and G. Qian, *Analyst*, 2011, **136**, 5283–5286.
18 L. Zhang, H. Chen, Z. Li, Z. Lu and R. Wang, *Inorg. Chem. Commun.*, 2012, **23**, 67–69.
19 X. Meng, S. Wang, Y. Li, M. Zhu and Q. Guo, *Chem. Commun.*, 2012, **48**, 4196–4198.
20 K. Sreenath, J. R. Allen, M. W. Davidson and L. Zhu, *Chem. Commun.*, 2011, **47**, 11730–11732.

21 Z. Xu, K.-H. Baek, H. N. Kim, J. Cui, X. Qian, D. R. Spring, I. Shin and J. Yoon, *J. Am. Chem. Soc.*, 2009, **132**, 601–610.

22 T. Cheng, T. Wang, W. Zhu, X. Chen, Y. Yang, Y. Xu and X. Qian, *Org. Lett.*, 2011, **13**, 3656–3659.

23 H. Tian, B. Li, J. Zhu, H. Wang, Y. Li, J. Xu, J. Wang, W. Wang, Z. Sun, W. Liu, X. Huang, X. Yan, Q. Wang, X. Yao and Y. Tang, *Dalton Trans.*, 2012, **41**, 2060–2065.

24 Y. Pourghaz, P. Dongare, D. W. Thompson and Y. Zhao, *Chem. Commun.*, 2011, **47**, 11014–11016.

25 S. Yin, J. Zhang, H. Feng, Z. Zhao, L. Xu, H. Qiu and B. Tang, *Dyes Pigm.*, 2012, **95**, 174–179.

26 H. M. Kim, M. S. Seo, M. J. An, J. H. Hong, Y. S. Tian, J. H. Choi, O. Kwon, K. J. Lee and B. R. Cho, *Angew. Chem., Int. Ed.*, 2008, **47**, 5167–5170.

27 X. Chen, J. Shi, Y. Li, F. Wang, X. Wu, Q. Guo and L. Liu, *Org. Lett.*, 2009, **11**, 4426–4429.

28 N. Y. Baek, C. H. Heo, C. S. Lim, G. Masanta, B. R. Cho and H. M. Kim, *Chem. Commun.*, 2012, **48**, 4546–4548.

29 G. Masanta, C. S. Lim, H. J. Kim, J. H. Han, H. M. Kim and B. R. Cho, *J. Am. Chem. Soc.*, 2011, **133**, 5698–5700.

30 S. Doose, H. Neuweiler and M. Sauer, *ChemPhysChem*, 2009, **10**, 1389–1398.

31 A. P. de Silva, H. Q. N. Gunaratne, T. Gunnlaugsson, A. J. M. Huxley, C. P. McCoy, J. T. Rademacher and T. E. Rice, *Chem. Rev.*, 1997, **97**, 1515–1566.

32 J. Wu, W. Liu, J. Ge, H. Zhang and P. Wang, *Chem. Soc. Rev.*, 2011, **40**, 3483–3495.

33 D. W. Domaille, E. L. Que and C. J. Chang, *Nat. Chem. Biol.*, 2008, **4**, 168–175.

34 L. Xue, C. Liu and H. Jiang, *Org. Lett.*, 2009, **11**, 1655–1658.

35 L. Xue, Q. Liu and H. Jiang, *Org. Lett.*, 2009, **11**, 3454–3457.

36 Y. Tan, J. Yu, J. Gao, Y. Cui, Z. Wang, Y. Yang and G. Qian, *RSC Adv.*, 2013, **3**, 4872–4875.

37 H. M. Kim and B. R. Cho, *Acc. Chem. Res.*, 2009, **42**, 863–872.

38 B. Zhu, C. Gao, Y. Zhao, C. Liu, Y. Li, Q. Wei, Z. Ma, B. Du and X. Zhang, *Chem. Commun.*, 2011, **47**, 8656–8658.

39 D. M. Nguyen, A. Frazer, L. Rodriguez and K. D. Belfield, *Chem. Mater.*, 2010, **22**, 3472–3481.

40 N. Karton-Lifshin, L. Albertazzi, M. Bendikov, P. S. Baran and D. Shabat, *J. Am.Chem. Soc.*, 2012, **134**, 20412–20420.

41 J. H. Delcamp, Y. Shi, J. H. Yum, T. Sajoto, E. Dell'orto, S. Barlow, M. K. Nazeeruddin, S. R. Marder and M. Gratzel, *Chem.–Eur. J.*, 2013, **19**, 1819–1827.

42 Y. Tan, Q. Zhang, J. Yu, X. Zhao, Y. Tian, Y. Cui, X. Hao, Y. Yang and G. Qian, *Dyes Pigm.*, 2013, **97**, 58–64.

43 Y.-Y. Wu, Y. Chen, G.-Z. Gou, W.-H. Mu, X.-J. Lv, M.-L. Du and W.-F. Fu, *Org. Lett.*, 2012, **14**, 5226–5229.

44 S. Rihn, P. Retailleau, A. De Nicola, G. Ulrich and R. Ziessel, *J. Org. Chem.*, 2012, **77**, 8851–8863.

45 A. Poirel, A. De Nicola and R. Ziessel, *Org. Lett.*, 2012, **14**, 5696–5699.

46 A. C. Benniston, T. P. Winstanley, H. Lemmetyinen, N. V. Tkachenko, R. W. Harrington and C. Wills, *Org. Lett.*, 2012, **14**, 1374–1377.

47 W. J. Hehre, *J. Chem. Phys.*, 1972, **56**, 2257.

48 A. D. Becke, *J. Chem. Phys.*, 1993, **98**, 5648–5652.

49 M. Cossi, N. Rega, G. Scalmani and V. Barone, *J. Comput. Chem.*, 2003, **24**, 669–681.

50 J. Tomasi, B. Mennucci and R. Cammi, *Chem. Rev.*, 2005, **105**, 2999–3094.

51 M. J. Frisch, G. W. Trucks, H. B. Schlegel, G. E. Scuseria, M. A. Robb, J. R. Cheeseman, G. Scalmani, V. Barone, B. Mennucci, G. A. Petersson, H. Nakatsuji, M. Caricato, X. Li, H. P. Hratchian, A. F. Izmaylov, J. Bloino, G. Zheng, J. L. Sonnenberg, M. Hada, M. Ehara, K. Toyota, R. Fukuda, J. Hasegawa, M. Ishida, T. Nakajima, Y. Honda, O. Kitao, H. Nakai, T. Vreven, J. A. Montgomery Jr., J. E. Peralta, F. Ogliaro, M. Bearpark, J. J. Heyd, E. Brothers, K. N. Kudin, V. N. Staroverov, R. Kobayashi, J. Normand, K. Raghavachari, A. Rendell, J. C. Burant, S. S. Iyengar, J. Tomasi, M. Cossi, N. Rega, J. M. Millam, M. Klene, J. E. Knox, J. B. Cross, V. Bakken, C. Adamo, J. Jaramillo, R. Gomperts, R. E. Stratmann, O. Yazyev, A. J. Austin, R. Cammi, C. Pomelli, J. W. Ochterski, R. L. Martin, K. Morokuma, V. G. Zakrzewski, G. A. Voth, P. Salvador, J. J. Dannenberg, S. Dapprich, A. D. Daniels, Ö. Farkas, J. B. Foresman, J. V. Ortiz, J. Cioslowski and D. J. Fox, *GAUSSIAN 09 (Revision A.1)*, Gaussian, Inc., Wallingford, CT, 2009.

52 A. Marini, A. Muñoz-Losa, A. Biancardi and B. Mennucci, *J. Phys. Chem. B*, 2010, **114**, 17128–17135.

53 A. A. Vasilev, K. De Mey, I. Asselberghs, K. Clays, B. Champagne, S. E. Angelova, M. I. Spassova, C. Li and K. Müllen, *J. Phys. Chem. C*, 2012, **116**, 22711–22719.

54 Y. Chen, C. Zhu, Z. Yang, J. Li, Y. Jiao, W. He, J. Chen and Z. Guo, *Chem. Commun.*, 2012, **48**, 5094–5096.